Regional Studies in Marine Science 78 (2024) 103775

Contents lists available at ScienceDirect

Regional Studies in Marine Science

journal homepage: www.elsevier.com/locate/rsma

Seasonal changes in the protist communities of Hakodate Bay, southern Hokkaido, from 2020 to 2022

Yusuke Hamao [a], Kyosei Morimoto [a], Shoko Tatamisashi [b], Masahide Wakita [b], Akihide Kasai [a,c], Kohei Matsuno [a,c,*]

[a] Faculty/Graduate School of Fisheries Science, Hokkaido University, 3-1-1 Minato-cho, Hakodate, Hokkaido 041-8611, Japan
[b] Mutsu Institute for Oceanography, Japan Agency for Marine-Earth Science and Technology (JAMSTEC), 690 Kitasekine Sekine, Mutsu, Aomori 035-0022, Japan
[c] Arctic Research Centre, Hokkaido University, Kita-21 Nishi-11 Kita-ku, Sapporo, Hokkaido 001-0021, Japan

ARTICLE INFO

Keywords:
Coastal monitoring
Phytoplankton dynamics
Photosynthetic activity
Local fisheries

ABSTRACT

Hakodate Bay at the southern end of Hokkaido experiences physical and chemical environmental changes in the adjacent Tsugaru Strait. Harmful algal blooms have occurred since 2015. However, information on the response of protist community composition, photosynthetic activity to environmental variables or the mechanisms causing harmful blooms in the Hakodate Bay is lacking. We investigated the seasonal changes in the protist community using weekly sampling to reveal the relationship between the protist community and environmental variables in the Hakodate Bay. Based on cluster analysis, six groups were identified: Winter, Spring, Late Spring, Summer, Benthic, and *Karenia*. High *Fv/Fm* was seen in the Summer, Benthic and Spring groups supported by high nutrients, warm temperature and sufficient irradiance. From the Winter to Spring group, a species transition from low-temperature-adapting *Thalassiosira* spp. to *Chaetoceros* spp. was found. The Summer group comprised high salinity-tolerant species (the diatom *Leptocylindrus danicus* and dinoflagellate *Prorocentrum* spp.) because of high fluctuations in salinity due to precipitation. The other groups (Late Spring, Benthic, and *Karenia*) randomly filled the spaces between the three groups. The dinoflagellate *Scrippsiella* spp. was dominant in the Late Spring group because of accumulation by wind-driven currents. Because a strong relationship between benthic species and wind speed was exhibited, the Benthic group comprised benthic diatoms released into the water by mixing. The *Karenia* group was observed only from late August 2021 to early January 2022, when higher ammonium and lower light conditions (i.e., cloudy conditions) were detected. Owing to environmental conditions, diatom growth was restricted by low light intensity, whereas that of *Karenia mikimotoi* increased by taking advantage of the abundant nutrients. Seasonal changes in the protist community of the Hakodate Bay can generally be explained by temperature; however, in the short term (1–2 weeks), changes were also influenced by meteorological conditions (solar radiation, wind, and precipitation).

1. Introduction

Phytoplanktons are important organisms responsible for primary production in marine ecosystems. As planktonic protists, diatoms, dinoflagellates, and euglenoids are the dominant taxa in the oceans. Diatoms are the main constituents of micro-sized phytoplankton communities, and their growth rates vary depending on temperature and nutrient concentrations (Sergeeva et al., 2010; Giesbrecht et al., 2019). Species-specific differences are present in physiological activity; half-saturation constants for the nitrate uptake rate are high for large species, such as *Thalassiosira* spp., and low for small species, such as *Chaetoceros* spp. (Eppley et al., 1969; Turpin and Harrison, 1980). In addition, the preferred water temperature differs among species; for example, *Thalassiosira* spp. prefer low water temperatures (Durbin, 1974). Diatoms exhibit a unique physiology with many species responding to environments unsuitable for growth by forming resting cells and settling on the sea floor (Hargraves and French, 1983; McQuoid and Hobson, 1996). These resting cells are highly durable, germinate mainly through light irradiation, and proliferate in suitable environments (Itakura, 2000). Diatoms are classified as pelagic or benthic based on their habitat. The habitats of benthic diatoms are limited to substrates in the photic layer; therefore, they are often found in shallow coastal

* Corresponding author at: Faculty/Graduate School of Fisheries Science, Hokkaido University, 3-1-1 Minato-cho, Hakodate, Hokkaido 041-8611, Japan.
E-mail address: k.matsuno@fish.hokudai.ac.jp (K. Matsuno).

https://doi.org/10.1016/j.rsma.2024.103775
Received 3 June 2024; Received in revised form 20 August 2024; Accepted 21 August 2024
Available online 27 August 2024

areas (Cadée and Hegeman, 1974).

Dinoflagellates are major constituents of phytoplankton communities and are classified into three types depending on their nutritional modes: autotrophic, mixotrophic, and heterotrophic (Elbrachter, 1991; Sanders, 1991). Autotrophic and mixotrophic dinoflagellates are the second most important producers in the classical grazing food chain (Raymont, 1980), and heterotrophic dinoflagellates act as microzooplankton, increasing in particle size from pico-nano to micro in the microbial food chain (Sherr and Sherr, 1988). The seasonal pattern of dinoflagellates differs from that of diatoms; in Funka Bay, Hokkaido, autotrophic and mixotrophic species occurred at high densities in an environment depleted of inorganic nutrients after the spring diatom bloom (Miyazono and Shimada, 2000). In addition, some dinoflagellates form cysts during their life cycle, which play an important role in expanding the distribution of the species, initiating and ending blooms, and surviving in unsuitable environments (Wall, 1971; Anderson, 1984; Steidinger, 1993). As a notable aspect of this taxon, some dinoflagellate species are classified as harmful algal blooms and cause damage to fisheries by forming red tides, which is a problem not only in Japan but also worldwide (Oh et al., 2005).

The warm and high-salinity Tsushima Warm Current flows into the southern coastal area of Hokkaido on the coast of the Sea of Japan. The flow volume changes seasonally, being low from March to May and peaking from August to November (Sato, 2001; Yasui et al., 2022). The Tsugaru Warm Current, which is a branch of the Tsushima Warm Current, also has high temperature and salinity. It flows into the Tsugaru Strait from the west entrance throughout the year and spreads across the Hakodate Bay at the southern end of Hokkaido throughout most of the year (Nishida et al., 2003). In contrast, from autumn to winter, the cold, low-salinity coastal Oyashio originates from the east entrance of the strait along the Hokkaido coast and occasionally reaches the Hakodate Bay (Ohtani, 1987). In recent years, changes have been observed in these ocean currents, and the flow volumes of the Tsushima Warm Current and Tsugaru Warm Water are reported to be increasing annually (Kida et al., 2021).

Because responses to environmental changes such as water temperature, salinity, and nutrient concentrations differ among protist species (Olli et al., 1996; Li et al., 2011; Liu et al., 2011; Karthik et al., 2017), protist community composition is considered an indicator of environmental change (e.g., Tadokoro et al., 2008). For example, in Japan, the dominant species has shifted from *Skeletonema* spp. to *Chaetoceros* spp., which was associated with decreased dissolved inorganic nitrogen (DIN) in Harimanada, Japan (Nishikawa et al., 2010). Red tides caused by *Karenia mikimotoi* occurred in the Hakodate Bay for the first time in 2015, and the mortality of fish and shellfish, such as salmon, Japanese common squid, and Ezo abalone, was recorded (Shimada et al., 2016; Kakumu et al., 2018; Shimada, 2021). The harmful species are believed to be transported by the Tsushima Warm Current with warming and increasing volume (Shimada et al., 2016; Kakumu et al., 2018). The dinoflagellate *Alexandrium pacificum*, which cause paralytic shellfish poisoning, and raphidophyte *Heterosigma akashiwo* are also found in the bay (Natsuike et al., 2019, 2021). On the other hand, several phytoplankton studies have been reported for the southern coastal area of Hokkaido, including species composition during spring blooms in the Iwanai Bay (Odate et al., 1993) and long-term changes in phytoplankton communities using net sampling in the Oshoro Bay (Fukui et al., 2010). However, information on the relationship between environmental variables and the entire protist community or the mechanisms causing harmful blooms in the Hakodate Bay is lacking.

As another aspect of phytoplankton response to environmental changes, stress conditions and photosynthesis activity in cells are useful parameters (Schreiber et al., 1995). To measure these, a pulse amplitude modulation (PAM) fluorescence method (Schreiber et al., 1986) is broadly used in field investigations because this method has the advantage that measurements can be made in a short time and non-destructively. The most commonly used parameter is the maximum quantum yield (*Fv/Fm*), which indicates the photochemical reaction per unit of light absorbed by chlorophyll in photosystem II (Schreiber et al., 1986). *Fv/Fm* has a maximum value of 0.8–0.83 in healthy cells and is used as an index of photoinhibition and temperature or nutrient stress tolerance (Björkman and Demmig, 1987; Goto et al., 2008). For example, under low-temperature conditions, the viscosity of the cell membrane decreases, suppressing photochemical reactions in the electron transport chain and resulting in a decrease in *Fv/Fm* (Morgan-Kiss et al., 2006). Additionally, using a light-curve function in PAM, the electron transport rate (ETR) can be estimated (Ohara et al., 2020). However, as well as the response in community composition, seasonality in the photosynthetic activity is not investigated in the Hakodate Bay.

In the present study, we aimed to investigate seasonal changes in the protist community and photosynthetic activity based on weekly sampling, and to reveal the response in the protist community and its activity by environmental variables in the Hakodate Bay.

2. Materials and methods

2.1. Sampling station

The fixed sampling station (41°48′42″ N, 140°42′11″ E) borders the No. 3 Sand Protection Dike in Nanaehama (Fig. 1). Nanaehama, located outside the port of Hakodate Bay and facing the Tsugaru Strait, is a shallow (1–2 m in depth) sandy beach. This area is a locally important fishing ground for flathead flounder and surf clams (Nakagami et al., 2001). The research site, Nanaehama No. 3 Sand Protection Dike, is divided into two areas: inside and outside the Hakodate Port, and the fluctuation characteristics of ocean currents and water quality ae known to differ between the inside and outside Hakodate Port (Miyatake et al., 2011). The area inside the port is more closed and more likely to accumulate nutrients, whereas the area outside the port is less closed and more susceptible to the influence of offshore water (Miyatake et al., 2011). Large amounts of nutrients flow into Nanaehama from outside the port because of increased river water associated with precipitation (Miyatake et al., 2011).

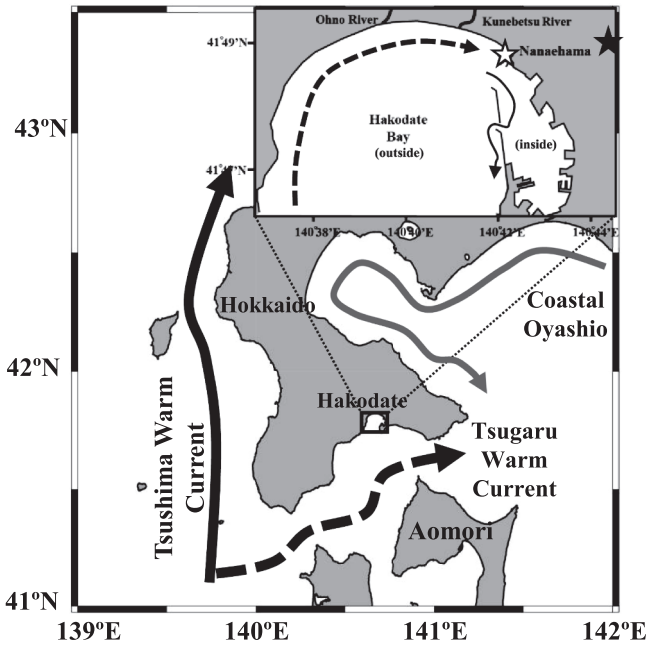

Fig. 1. Location of the sampling station (open star, Nanaehama) in the Hakodate Bay, southern Hokkaido. Solid star indicates the Hakodate meteorological station. Arrows indicate the main current around the sampling area.

2.2. Meteorological data

Meteorological data at the Hakodate meteorological station (Fig. 1), including daily average temperature (°C), daily total precipitation (mm d^{-1}), scalar average wind speed and most-frequent wind direction, daylight hours (h), and daily total solar radiation (MJ m^{-2} day^{-1}) were obtained from the Japan Meteorological Agency website (https://www.data.jma.go.jp/gmd/risk/obsdl/index.php). The research period was two years, from September 1, 2020 to August 31, 2022.

2.3. Field sampling

Weekly sampling was conducted (104 sampling events) outside the No. 3 Sand Protection Dike in Nanaehama from September 3, 2020 to August 26, 2022. The sampling time was 13:00–14:00. One liter of surface seawater was collected for phytoplankton analysis using a plastic bucket. Water samples were fixed with glutaraldehyde (final concentration 1 %) and stored in the dark. Separately, seawater was collected for measuring chlorophyll *a* concentration, nutrients concentration, and photosynthetic activity and brought back to the land laboratory in the dark. Water temperature and salinity were measured using three sensors (YSI-Pro30; Xylem Japan, Kawasaki, Japan, HORIBA; Horiba Advanced Techno, Kyoto, Japan, AAQ-RINKO; JFE Advantech, Nishinomiya, Japan). Starting in April 2021, the turbidity in water and photosynthetic photon flux density (PPFD) in air were measured using a turbidity sensor (TD-M500, Optex) and a light analyzer (LA-105, Nippon Medical Instruments Manufacturing Co., Ltd.), respectively. The turbidity probe was sunk into seawater collected by a bucket, waited for a while, and then measured the turbidity. Regarding PPFD, dark calibration was conducted every time before the *in-situ* measurement, and the light sensor instantaneously measured PPFD without any artificial shade.

2.4. Sample analysis

Water samples for nutrient analysis were frozen at −80°C until measurement. After thawing, the nitrate, nitrite, ammonium, phosphate, and silicate concentrations were measured using an autoanalyzer (QuAAtro 2HR, BL-TEC, Tokyo, Japan) (Wakita et al., 2021). For chlorophyll *a*, 100–1000 mL of seawater was filtered through a GF/F filter and extracted with 6 mL of N,N-dimethylformamide. The chlorophyll *a* concentration was measured by the method of Holm-Hansen et al. (1965) using a Turner fluorometer (10-AU; Turner Designs).

Photosynthetic activity was measured in fresh samples from February 28, 2022, to August 26, 2022, using a pulse amplitude modulation (PAM) fluorometer (Water-PAM; Heinz Walz, PAM-CONTROL, Germany). Fresh seawater (4.0 mL) was placed into the glass cell, inserted into the emitter-detector unit, and the *Ft* value was adjusted within the range of 200–300 by adjusting the PM-Gain. After dark adaptation for 15 min or more, fluorescence values F_0 (when irradiated with only a sufficiently weak pulsed measurement light) and *Fm* (when the primary quinone electron acceptor (Q_A) of photosystem II was rapidly reduced by irradiation with excitation light) were measured. The maximum quantum yield (Fv ($=Fm - F_0$) $/Fm$) of photosystem II was calculated. After a further dark adaptation of more than 15 min, the relative electron transport rate (rETR) was measured using the light curve function on eight levels of excitation light (92, 138, 209, 307, 467, 694, 980, and 1352 μmol photons m^{-2} s^{-1}). Finally, the initial slope (alpha) and maximum electron transfer rate (ETRm) of the rETR curve were calculated from the obtained photo-electron transfer rate curve.

Fixed samples (1 L) were stored on a stone table for more than 1 d to allow the phytoplankton cells to settle at the bottom of the bottle. Subsequently, the samples were concentrated to 20 mL by using a siphon. Subsamples (500 μL) of the concentrated sample were mounted on a glass slide using a micropipette. Microsized cells were identified and enumerated using an inverted microscope (ECLIPSE Ts2R, Nikon) at 40–600× magnification. Diatoms were identified to the lowest possible level (species or genus) according to Hasle and Syvertsen (1997), Horner (2002), and Al-Yamani and Saburova (2011). Dinoflagellates were identified to the genus level according to Fukuyo et al. (1997) and Steidinger and Tangen (1997). Silicoflagellates, prasinophytes, and euglenoids were identified to the species or genus level according to Throndsen (1997). Tintinnid and oligotrich ciliates were counted separately. When red tides of the raphidophyte *H. akashiwo* were observed on June 7, 2021 and July 1, 2022, species identification and counting were performed using fresh samples. Note that our fixation (glutaraldehyde) is an adequate fixative for diatoms and armored dinoflagellates but not for naked dinoflagellates and ciliates (Stoecker et al., 1994). Due to that, our fixation may have biased the community composition. Cells were counted at a maximum of 300 cells per sample, following which the cell density (cells L^{-1}) was calculated.

2.5. Data analysis

To reduce the bias for abundant species, the cell density data (X: cells L^{-1}) for each taxon, genus, and species were transformed to $\sqrt[4]{X}$ before cluster analysis (Quinn and Keough, 2002). Similarities between samples were examined using the Bray–Curtis index based on differences in species composition. The similarity indices were coupled to group the samples using hierarchical agglomerative clustering with a complete linkage method, the unweighted pair group method with arithmetic mean. Similarity profile analysis (SIMPROF) was conducted to determine whether the groupings of stations were statistically significant (at a 5 % significance level). Based on the fourth root-transformed cell density, a similarity percentage (SIMPER) analysis was applied to determine which species contributed to the top 50 % of the total abundance of each group. To identify potential indicator species in the groups resulting from the cluster analysis, the Indicator Value (IndVal) program was applied (Dufréne and Legendre, 1997). The relationship between each sample and the normalized environmental data (water temperature, salinity, DIN, phosphate, silicate, DIN/P, Si/P, daily average temperature, daily total precipitation, daily average wind speed, daylight hours, and daily total solar radiation) was evaluated using distance-based linear modeling (DistLM) and redundancy analysis (RDA). To run DistLM, we chose “Step-wise” as the selection procedure, “AICc” as the selection criterion, and the number of permutations was 999. Cluster analysis, DistLM, and RDA were conducted using the Primer 7 software (PRIMER-E Ltd., Albany, Auckland, New Zealand).

Differences in environmental parameters (water temperature, salinity, DIN, phosphate, silicate, DIN/P, Si/P, daily average temperature, daily total precipitation, daily average wind speed, daylight hours, and daily total solar radiation) among the groups (identified by cluster analysis based on protist cell density) were tested using the Max-t method with heteroscedastic consistent covariance estimation (HC3) (Herberich et al., 2010). The tests were conducted using R software with the packages “multcomp” and “sandwich” (version 4.1.2; R Core Team, 2021).

To test the effect of physical disturbances on benthic diatoms, the relationship between cell density and environmental factors (turbidity and wind speed) was analyzed using generalized linier models (GLMs). Data were collected from April 2021 to August 2022 when turbidity was observed. Variance inflation factors (VIF) (Zuur et al., 2009) were calculated to remove multicollinearity among the environmental parameters. Because all VIF values were below 3, none of the parameters were removed from the subsequent analysis. Next, a full model was constructed with benthic diatom cell density as the response variable, and turbidity and wind speed as explanatory variables. To run the GLMs, we used a negative binomial distribution based on raw count data, with the analyzed subsample volumes and concentration factors (from 1 L to 20 mL) applied as an offset. The GLMs were conducted using R software with the package “MASS” (version 4.1.2; R Core Team, 2021).

Based on the photosynthetic activity data (*Fv/Fm*, alpha, and ETRm)

measured with PAM, the ETR per unit volume (ETR, μmol electron m^{-3} s^{-1}) at each sampling was calculated using the following procedure. First, the PPFD incident on the sea surface was calculated by multiplying the PPFD measured in the field by 0.85 (Parsons et al., 1984). Next, alpha and ETRm were measured using the light curve function, and the PPFD incident on the sea surface was substituted into Eq. (1) to obtain rETR.

$$rETR = ETRm \times \tanh(alpha \times PPFD \times ETR\ m^{-1}) \quad (1)$$

Next, a*, the absorption coefficient specific to chlorophyll *a*, was determined using Eq. (2) (Bricaud et al., 1995).

$$a^*\ (m^2\ mg\ Chl.\ a^{-1}) = 0.0403 \times \textit{in-situ}\ \text{chlorophyll } a \text{ concentration (mg } m^{-3})^{(-0.332)} \quad (2)$$

Using rETR and a*, ETR (μmol electron mg chl. $^{-1}$ s^{-1}) per chlorophyll *a* was calculated using Eq. (3).

$$ETR = rETR \times 0.768 \times a^* \quad (3)$$

The constant 0.768 in this equation is the photon absorption rate in photosystem II (Johnsen and Sakshang, 2007).

Finally, the ETR per unit volume (μmol electron m^{-3} sec^{-1}) was determined by multiplying the ETR per chlorophyll *a* by the *in-situ* chlorophyll *a* concentration. Additionally, to evaluate the photosynthetic activity of each community divided by cluster analysis in response to light intensity, the average values of alpha and ETRm for each community were substituted into Eq. (1) to create a light-electron transfer rate curve.

3. Results

3.1. Hydrographic and meteorological variables

The temperature ranged from 4.5−27.3°C with regular seasonal changes (Fig. 2). Salinity ranged from 18.0−33.6 with frequently dropped down below 30 (25 % in frequency), particularly for distinct decreases (below 25) in early November 2020, late August 2021, and August 2022. Chlorophyll *a* concentration ranged from 0.11−181.2 μg L^{-1} and exhibited high values from March to November 2021 and July 2022 (Fig. 2). DIN and silicate ranged from 4.3−62.6 μM and 3.9−155.9 μM, respectively, with clear peaks when salinity decreased drastically. Phosphate ranged from 0.3 to 6.8 μM with a peak on July 1, 2022. The DIN/P ratio was 2.1−112.6, with peaks in March and June 2022. The Si/P ratio was 7.3−225.0 and increased when salinity decreased drastically. Turbidity ranged from 1.2 to 110 (FTU), with peaks on June 7, 2021 and July 1, 2022. The values for PPFD ranged from 37.06 to 2239 μmol m^{-2} s^{-1}. Air temperature ranged from −10.1–27.2°C, and warm conditions were observed in August and September 2020 and July 2021. Precipitation exhibited a range from 0 to 104.5 mm d^{-1}. Daily total solar radiation ranged from 1.5 to 28.95 MJ m^{-2} day^{-1} with similar seasonality to temperature. Wind speed was 1.5−9.9 m s^{-1}, and northwest and southeast winds were dominant in winter (November to March) and summer (May to August), respectively. The east-west component was usually higher than the north-south component.

3.2. Seasonal changes in protists

Cell densities of diatoms, dinoflagellates, ciliates, and euglenoids were 7.53×10^3−6.00×10^5 cells L^{-1}, not detected (N.D.) −1.40×10^6 cells L^{-1}, N.D.−4.17×10^4 cells L^{-1}, and N.D.−1.39×10^5 cells L^{-1}, respectively (Fig. 3a). Diatoms constantly occurred at a high density (1.0×10^4−1.0×10^6 cells L^{-1}). In contrast, dinoflagellates, ciliates, and euglenoid algae exhibited normal seasonality; cell density decreased from September 2020 to February 2021, increased from May to October 2021, decreased from November 2021 to March 2022, and then increased again (Fig. 3a). Regarding diatom species composition, *Thalassiosira* spp. was dominant from January to March (Fig. 3b). During the other periods, from early October to late December 2020, *Melosira* spp. and other pennate diatoms, and from March 2021 onwards, *Chaetoceros* spp., *Melosira* spp., and *Pseudo-nitzschia* spp., and other pennate diatoms were dominant (Fig. 3b). As an occasional change, the raphidophyte *H. akashiwo* occurred at a high density on June 7, 2021 and July 1, 2022 (Fig. 3b).

3.3. Relationship between protist community composition and environmental variables

In this study, 86 species belonging to 49 genera of diatoms, 12 genera (including two species) of dinoflagellates and oligotrich and tintinnid ciliates, one genus and two species of euglenoids, one genus of silicoflagellates, one genus of prasinophytes, and one species of raphidophytes were identified (Supplementary Table 1). Among the diatoms, 28 genera and 35 species were benthic. Cluster analysis based on cell density showed that the microplankton communities were divided into six groups (Summer, Late Spring, Benthic, Winter, Spring, and *Karenia*) with similarities between 35.6 % and 40.6 % (Fig. 4a). The Summer group mainly occurred from early June to late September (Fig. 4b) and was dominated by dinoflagellates and *Chaetoceros* spp.; the diatoms *Chaetoceros socialis*, *Cylindrotheca closterium*, *L. danicus*, *Navicula* spp., *Skeletonema costatum*, and the dinoflagellate *Prorocentrum* spp. were the characteristic species (Fig. 4c, Supplementary Table 1). The Late Spring group occurred from May to June and October 2021 and was dominated by dinoflagellates, with the diatom *Melosira varians* and dinoflagellate *Scrippsiella* spp. being the characteristic species (Fig. 4c, Supplementary Table 1). The Benthic group occurred from March to June, August, and October to late November and was dominated by *Melosira* spp. and other pennate diatoms, whereas *Grammatophora oceanica*, *M. varians*, and *Navicula* spp. were the characteristic species (Fig. 4c, Supplementary Table 1). The Winter group mainly occurred during the winter season from late November to early March; however, in 2022, owing to the appearance of *K. mikimotoi*, the group was seen later, from mid-January compared to during 2020–2021. This group exhibited the lowest average total cell density, and the diatom *Thalassiosira* spp. was dominant (Fig. 4c). The diatoms *Cocconeis* spp., *Navicula* spp., *Thalassiosira gravida*, and *Thalassiosira nordenskioeldii* were characteristic species in this group (Fig. 4c, Supplementary Table 1). The Spring group occurred from mid-March to early May and was dominated by the diatoms *Chaetoceros* spp., with the diatoms *Chaetoceros curvisetus*, *C. debilis*, *Chaetoceros socialis*, *M. varians*, and *Navicula* spp. being the characteristic species. (Fig. 4c, Supplementary Table 1). The *Karenia* group occurred only from late August 2021 to early January 2022 and was dominated by the dinoflagellate *K. mikimotoi*, with the diatoms *M. varians* and *Navicula* spp., and oligotrich ciliates being the characteristic species (Fig. 4c, Supplementary Table 1). These communities were roughly classified using distance-based RDA (Fig. 4d). The Summer, Spring, Benthic, and Winter groups were distributed close to each other, whereas the other groups were randomly distributed. As the best solution for DistLM, four environmental parameters (water temperature, phosphate, air temperature, and wind speed) accounting for 22.2 % of protist variation, were selected from the 12 evaluated parameters.

Water temperature, chlorophyll *a*, phosphate, air temperature, precipitation, wind speed, and total solar radiation were significantly ($p < 0.05$) different among the groups (Table 1). Water and air temperatures were the highest in the Summer group and lowest in the Winter group. Phosphate levels were higher in the Late Spring and Benthic groups and lower in the Winter and Spring groups. The lowest precipitation was observed in the Spring group. High wind speed was seen in the Benthic group, while low values was in Late spring group. Total solar radiation was high in the Late Spring, Spring, Summer, and Benthic groups, and low in the Winter and *Karenia* groups (Table 1).

A GLM was performed on benthic diatoms using turbidity and wind

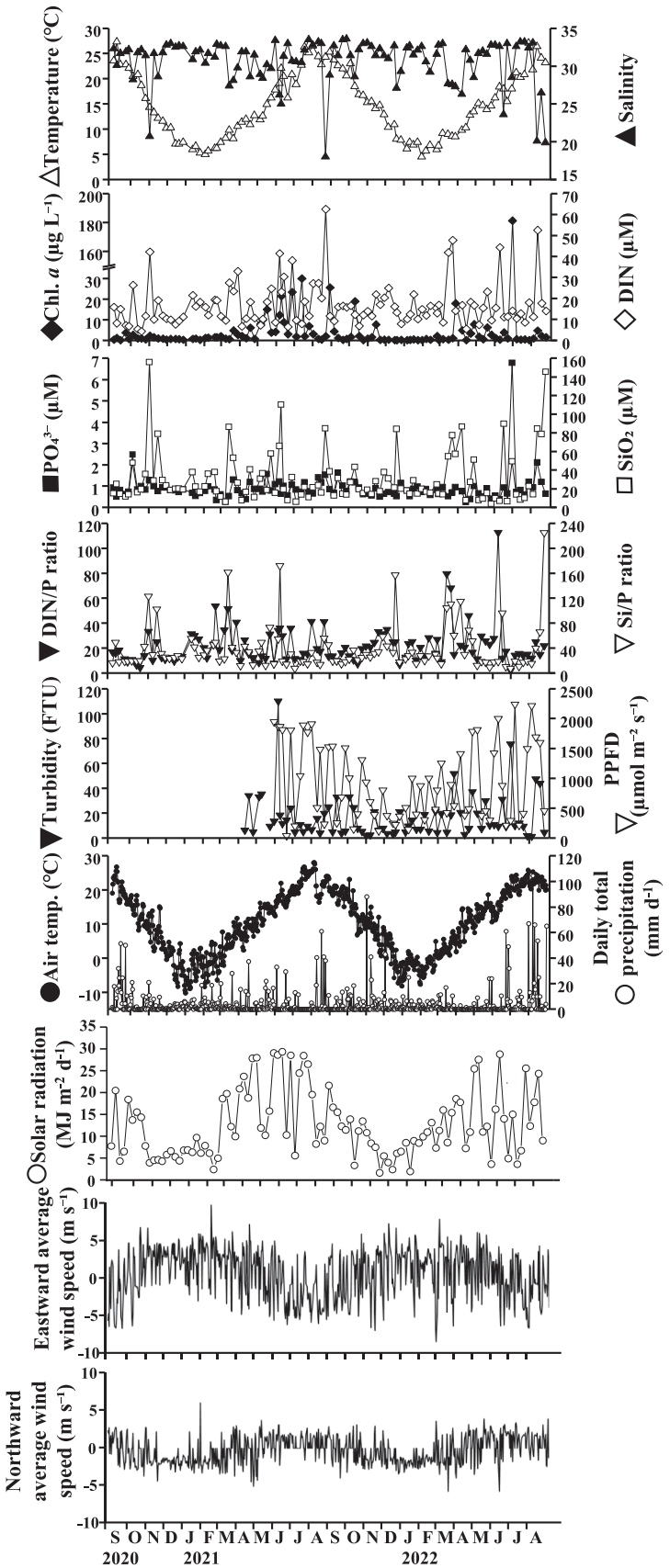

Fig. 2. Seasonal changes in environmental parameters (sea surface temperature, salinity, turbidity, photosynthetic photon flux density (PPFD), nutrients (dissolved inorganic nitrogen (DIN), PO_4^{3-}, SiO_2), DIN/P ratio, Si/P ratio, air temperature, daily total precipitation, daily total solar radiation, eastward and northward daily average wind speed) in the Hakodate Bay from September 2020 to August 2022.

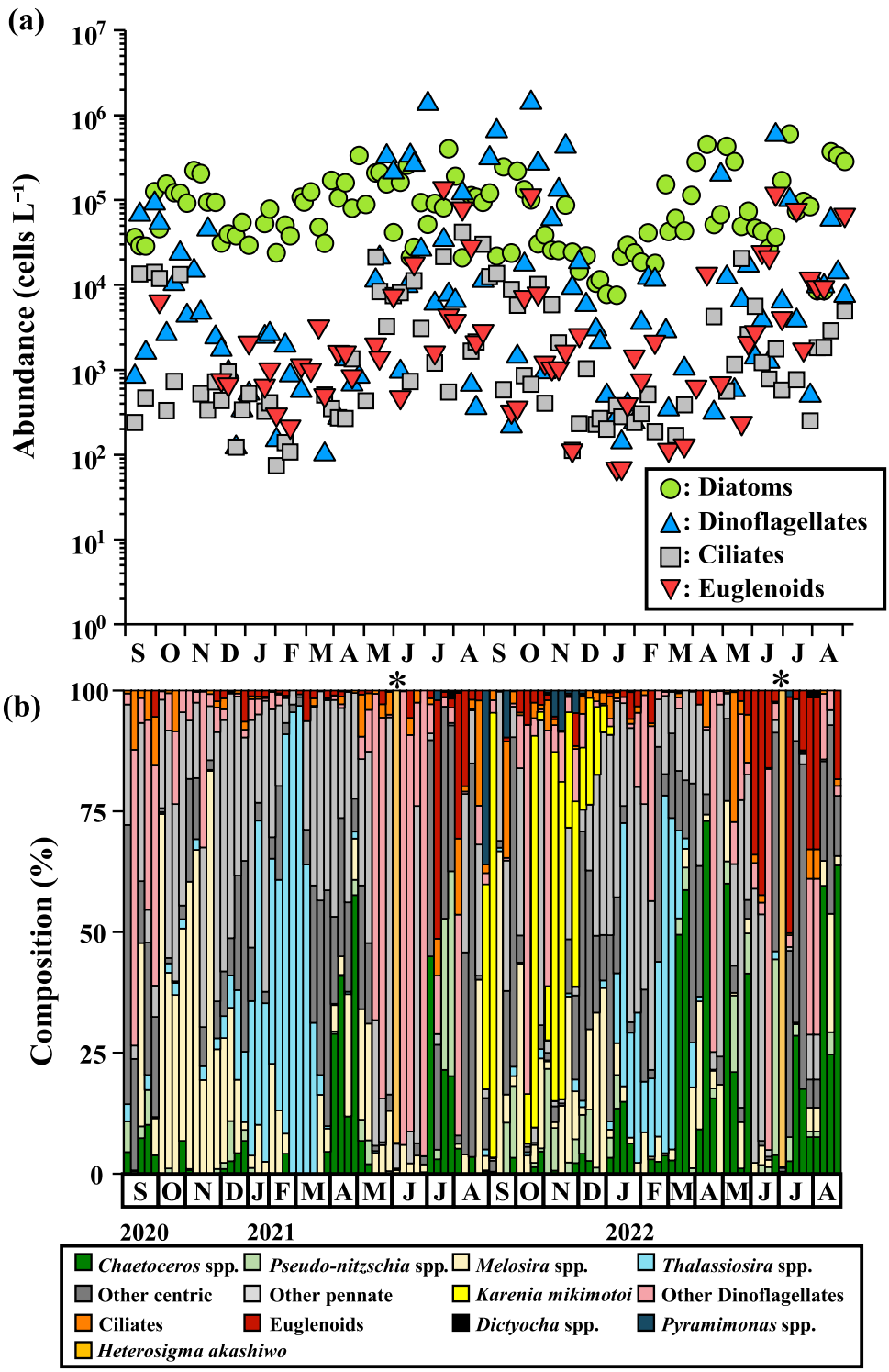

Fig. 3. Seasonal changes in protist abundance (a) and species composition (b) in the Hakodate Bay from September 2020 to August 2022. *: These data were removed from cluster analysis (cf. Fig. 4a).

speed as explanatory variables. The cell density of benthic diatoms increased when turbidity was high and the wind was strong (Table 2).

3.4. Photosynthetic activity

Regarding the photosynthetic activity index of each community, *Fv/Fm* was high at an average of >0.55 in the Summer (0.70), Benthic (0.64), and Spring (0.58) groups and low at <0.5 in the Late Spring (0.49) and Winter (0.48) groups (Fig. 5a). Note that the photosynthetic activity was not measured during the Karenia group. Alpha was high, with an average of >0.13 in the Late Spring (0.17) and Benthic (0.14) groups (Fig. 5b). The ETRm was high, with an average of >68, in the Late Spring (69) and Winter (76) groups but was low in the Summer (46), Benthic (47), and Spring (45) groups (Fig. 5c). The average ETR at the time of sampling was high in the Late Spring (5.0 μmol electron mg m^{-3} s^{-1}) and Benthic (4.1 μmol electron mg m^{-3} s^{-1}) groups. The lowest

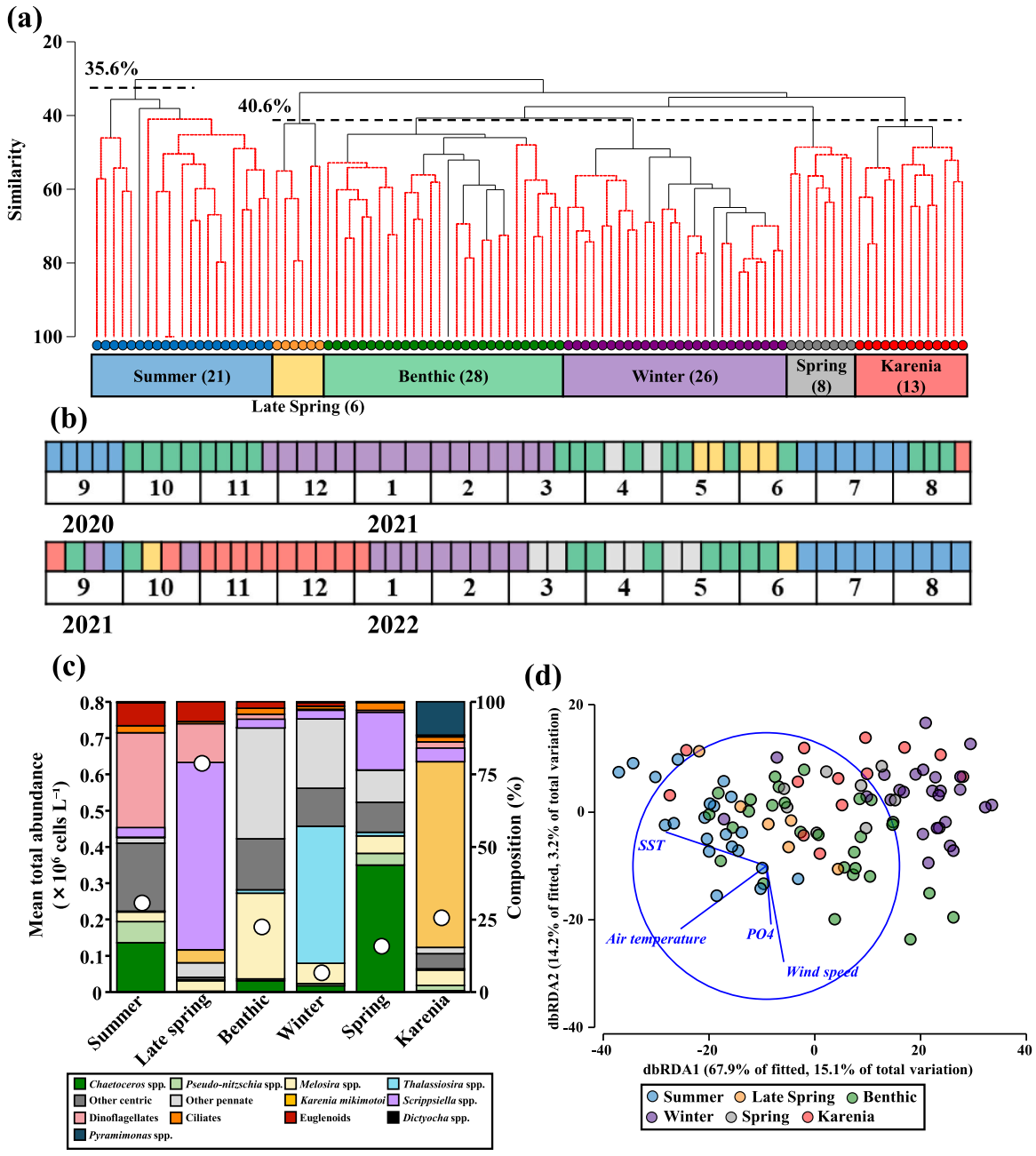

Fig. 4. Results of cluster analysis based on protist abundance by Bray–Curtis similarity associated with the unweighted pair group method with arithmetic mean (a). Six groups were identified with similarities between 35.6 % and 40.6 % (dashed lines). Numbers in the parentheses indicate the number of samples included in each group. Seasonal changes in the occurrence of the groups from September 2020 to August 2022 (b). Abundance and species composition of each group (c). Distance-based redundancy analysis (dbRDA) plot of the six groups with environmental parameters (d). The parameters were selected using distance-based linear modeling procedures consisting of step-wise, AICc (Akaike information criterion corrected for small samples), and 999 permutations. The direction of the lines indicates the relationship between groups and the parameters.

values were observed in the Summer (1.7), Winter (0.7), and Spring (1.3) groups (Fig. 5d). The light-ETR curves based on the average of alpha and ETRm values for each community exhibited similar shapes in the Summer, Benthic, and Spring groups. The maximum value of rETR was >600 μmol m^{-2} s^{-1} (Fig. 5e). The Late Spring group exhibited the highest ETR under weak-light conditions. In the Winter group, although the slope was flat, the maximum value under high light conditions (>1100 μmol m^{-2} s^{-1}) showed the highest ETR of all communities (Fig. 5e).

4. Discussion

4.1. Phytoplankton monitoring

In the coastal water, phytoplankton community is affecting by physical processes at various temporal scales, such as instantaneous surface wave, turbulence, daily tidal cycle, seasonal cycle, climate change (Dickey et al., 2001; Bi et al., 2022). From high-frequent *in-situ* imaging system, phytoplankton variability change from weekly to biweekly scales in a coastal area (Bi et al., 2022). In this study, seasonal cycle is mainly targeted, thus, weekly sampling is sufficient for evaluating that. On the other hand, as another concern in comparison

Table 1
Comparison of environmental factors between the groups identified by cluster analysis (cf. Fig. 4a) in the Hakodate Bay from September 2020 to August 2022. Different superscript numbers indicate significant ($p < 0.05$) differences between groups. The superscript alphabets are included only for significant variables by the Max-t test, and the order is from high to low alphabetically. Absence of a superscript alphabet means the inter-group difference in the variables was not significant. Values are mean ± S.D. Numbers in parentheses are the number of sampling dates belonging to each group.

Parameters	Groups					
	Summer (21)	Late Spring (6)	Benthic (28)	Winter (26)	Spring (8)	*Karenia* (13)
Temperature (°C)	22.9±2.98^{a}	18.4±2.66^{b}	15.7±4.92^{b,c}	8.0±3.74^{d}	11.9±2.43^{c}	14.0±5.75^{b,c}
Salinity	30.8±3.92	28.1±3.08	29.9±3.63	31.9±1.36	30.7±1.91	31.3±1.82
DIN (μM)	16.1±11.1	20.0±7.50	18.8±13.4	14.4±4.85	19.7±16.2	14.2±5.59
PO_4^{3-} (μM)	0.89±0.35^{a}	1.02±0.33^{a}	1.01±0.42^{a}	0.73±0.19^{a,b}	0.54±0.20^{b}	0.74±0.18^{a,b}
SiO_2 (μM)	28.0±34.0	56.6±37.4	37.4±32.6	22.8±15.1	26.6±25.9	27.9±18.8
DIN/P	17.7±7.90	21.8±11.7	20.9±20.3	21.9±11.6	36.7±25.6	20.7±9.35
Si/P	32.5±46.2	68.1±60.2	36.9±30.4	33.3±28.0	49.8±39.9	41.3±36.7
Chl. *a* (μg L^{-1})	4.10±7.79^{a}	12.0±7.61^{a}	3.50±3.84^{a}	0.71±0.55^{b}	1.1±1.01^{b}	3.4±7.06^{a,b}
Air temperature (°C)	21.3±3.16^{a}	16.6±1.66^{b}	12.3±5.48^{c}	0.47±6.01^{d}	9.0±5.09^{c}	7.4±8.47^{c,d}
Precipitation (mm d^{-1})	5.2±11.5^{a}	6.9±10.4^{a}	2.7±5.56^{a,b}	3.1±5.20^{a}	0.06±0.18^{b}	2.1±3.58^{a,b}
Wind speed (m s^{-1})	4.0±1.79^{a,b}	2.8±0.81^{b}	4.1±1.34^{a}	3.6±1.24^{a,b}	2.9±1.15^{a,b}	3.0±1.36^{a,b}
Solar radiation (MJ m^{-2} d^{-1})	15.2±8.69^{a}	16.7±10.3^{a}	13.8±7.45^{a}	8.7±4.48^{b}	16.4±8.46^{a}	8.4±5.65^{b}
Daylight hours (h)	5.5±4.94	5.2±6.06	5.1±4.06	4.4±3.39	6.1±5.64	4.4±2.94

Dissolved Inorganic Nitrogen: DIN.

Table 2
Result of GLM for benthic species (cf. Supplementary Table 1) abundance in the Hakodate Bay from September 2020 to August 2022. *: $p < 0.05$; ***: $p < 0.001$.

Variables	Estimate	Std.	Error	Z value	Pr (>|z|)
Intercept	8.96476	0.343247	26.118	< 2e−16	***
Turbidity	0.049466	0.007181	6.888	5.64E−12	***
Wind speed	0.214491	0.089029	2.409	0.016	*

between phytoplankton and hydrography, phytoplankton community structure could be an indicator in previous environmental condition in a few days, not the present condition. Although one day time-lag is known between temperature and chlorophyll *a* (Dickey et al., 2001), the time-lag effect was not evaluated due to our weekly sampling. To overcome the problem, more high-frequent dataset by mooring or modeling are needed.

4.2. Summer group

During summer (August–September), the velocity of the Tsugaru Warm Current increases, and its path is close to the sampling area (Yasui et al., 2022). Although the Tsugaru Warm Current is defined as having a water temperature of >5°C and a salinity of 33.7−34.2 (Hanawa and Mitsudera, 1987), the water temperature (15.5–27.3°C, average 22.9°C) was within the defined value during the entire period, whereas the salinity (19.9–33.6, average 30.8) was lower. This is because river water increased owing to precipitation, as the total daily precipitation was higher in September 2020, August 2021, and June–August 2022. High precipitation induces nutrients supply by river runoff (Sugimoto et al., 2021). Due to high irradiance and high nutrients, the highest *Fv/Fm* was seen during the Summer group (Goto et al., 2008). As another response in phytoplankton, the environmental characteristic may have induced the dominance of broad-haline species (diatoms *L. danicus* and *S. costatum* and dinoflagellate *Prorocentrum* spp.). *Leptocylindrus danicus* was reported to cause blooms in the Andaman Islands in eastern India after rapid freshening associated with large-scale precipitation (Karthik et al., 2017), whereas *S. costatum* can grow at salinities between 10 and 35 (Yamada, 2013). Regarding the dinoflagellate *Prorocentrum* spp., blooms of *Prorocentrum triestinum* have been confirmed in both the estuarine and inner bay areas on Nanji Island, China, suggesting that it has a wide range of salinity tolerances (Li et al., 2011). Therefore, during the occurrence period of the Summer group, the environmental conditions underwent drastic changes, such as the influx of high temperature, high-salinity Tsugaru Warm Current, and low salinity owing to precipitation, resulting in the dominance of *S. costatum*, *L. danicus*, and *Prorocentrum* spp., which could adapt to a wide range of environments.

4.3. Dominance of Scrippsiella spp. in the late spring group

The Late Spring group was observed in May and June but did not occur for over two consecutive weeks. This group was characterized by a high abundance of *Scrippsiella* spp. (4.0×10^5 cells L^{-1}). *Scrippsiella* spp. are autotrophic dinoflagellates that survive in unfavorable environments by forming cysts (e.g., Uchida, 1994). Cysts of *Scrippsiella trochoidea* germinated at water temperatures of 5, 10, 14, 18, and 22°C; however, all germinated cells died at 5°C, and at 10°C or higher, vegetative cells proliferated (Uchida, 1994). Although the cysts of this species in the sediments of Hakodate Bay were not investigated, it is suggested that this species was not transported by ocean currents such as the Tsushima Current, but instead formed cysts and established around Hakodate Bay, as they occurred in the water throughout the year. After germination from the cyst, the vegetative cells of this species actively grow at 14–22°C (Uchida, 1994). The water temperature during the occurrence period of the Late Spring group ranged from 14.9 to 22.1°C, corresponding to the suitable temperature for their growth.

The PAM measurement results showed that the Late Spring group had a slightly low *Fv/Fm*, high chlorophyll *a* concentration, alpha, and high ETR. This indicates that although the ETR in the water column was high, the physiological state of the cells deteriorated owing to high cell density. Regarding the influence of nutrient concentration on the growth of *Scrippsiella* spp., the nutrient concentrations during the Late Spring group were at the highest level among all groups: 56.6 μM for silicate, 20.0 μM for DIN, and 1.02 μM for phosphate. DIP < 0.1 μM and DIN/DIP > 22 are defined as phosphate depletion conditions for *Scrippsiella* spp. (Redfield et al., 1963; Brzezinski, 1985; Justic et al., 1995). In the Hakodate Bay, phosphate concentrations exceeded 0.1 μM during all sampling periods; however, in this study, DIN/DIP exceeded 22 on several days. This means that the growth of the species was not restricted by nutrients. Based on laboratory experiments, even when sufficient nutrients were added to a culture of *S. trochoidea* in a non-red tide state, cell density did not reach the cell density during red tides in nature (Yin et al., 2008). Therefore, increased nutrient concentrations increase the cell density of this species, but are not a direct factor in causing red tides, and the physical aggregation effect of wind is another contributing factor (Yin et al., 2008). Among the days when the Late Spring group occurred, the cell density of *Scrippsiella* spp. was significantly higher on October 11, 2021 (7.3×10^5 cells L^{-1}) and June 17, 2022 (5.5×10^5 cells L^{-1}) and the daily wind direction on those days was west-northwest. Because the west-northwest wind was almost directly in front of the sampling site (Nanaehama No. 3 Sand Protection Dike), it is possible

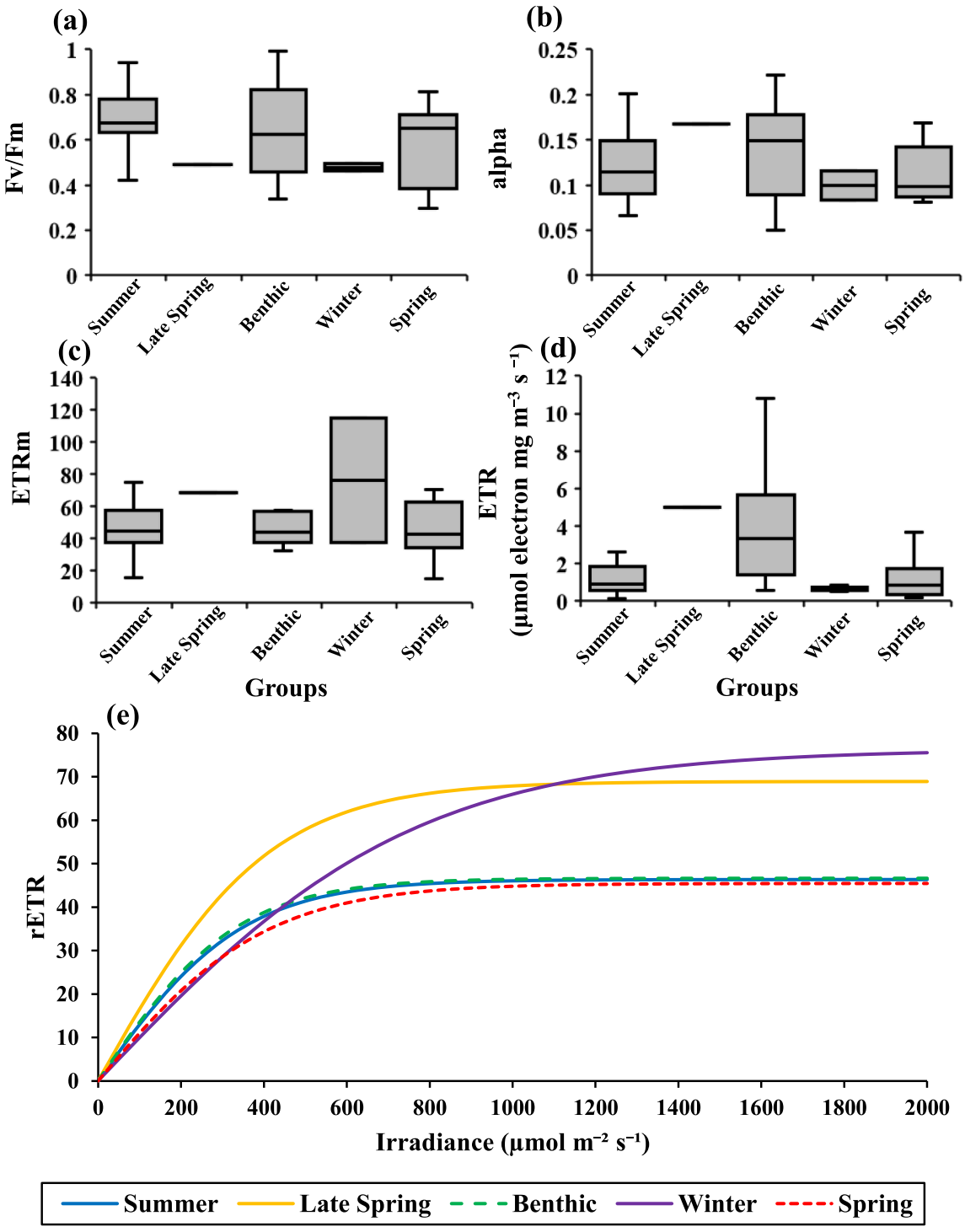

Fig. 5. Comparison of photosynthetic parameters (*Fv/Fm*, alpha, ETRm, and ETR) (a-d) based on PAM measurement among the groups identified a cluster analysis (cf. Fig. 4a) from February to August 2022. To estimate the ETR, PPFD and Chl. *a* concentration were used in each sampling (details in Materials and Methods). The light curve was estimated from the alpha and ETRm values in each group (e).

that *Scrippsiella* spp., was transported from offshore by wind-driven currents, accumulated around the sand protection levee. Thus, the cysts of *Scrippsiella* spp., which had been living in an unsuitable environment in the sediments around Hakodate Bay, germinated and grew with the increasing temperature and achieved a high cell density because of the high nutrient concentration and wind-driven currents.

In areas characterized by high DIN/DIP and phosphate deficiency, species transition from diatoms to dinoflagellates (Wei et al., 2004) and the occurrence of harmful algal blooms have been reported (Egge, 1998; Oh et al., 2005). *Scrippsiella trochoidea* is a harmless species. However, if it reaches high densities, it can cause a lack of dissolved oxygen, leading to fish death (Tian et al., 2021). If *Scrippsiella* spp. occur at a high density in Hakodate Bay, they may cause damage to local fisheries. Thus, the continuous investigation of nutrients, including phosphate and this species, is necessary.

4.4. Irregular occurrence of the benthic group

The Benthic group occurred irregularly in spring and autumn, and the characteristic species were benthic diatoms *G. oceanica*, *M. varians*, and *Navicula* spp. During the occurrence period of the Benthic group, the average wind speed was 4.1 m s^{-1}, and the average turbidity was 23.8 FTU, the highest values among all assemblages. The results of the GLM examining the effect of turbidity and wind speed on benthic diatom density showed that both variables had a significant effect: benthic diatoms increased when turbidity was high and the wind was strong. Therefore, it is speculated that underwater agitation associated with strong winds causes benthic and sessile diatoms to become suspended in the water from the bottom sediment and quay, thereby increasing the number of these diatoms.

Fv/Fm is an indicator of phytoplankton photosynthetic potential and nutrient limitation (DiTullio et al., 2000), and the maximum value for phytoplankton is reported to be 0.6−0.8 (Buchel and Wilhelm, 1993). Because *Fv/Fm* (0.64) in the benthic group was relatively high in the Hakodate Bay, benthic and sessile diatoms suspended in water likely contributed to this high photosynthetic activity. In the Puget Sound (Thom and Albright, 1992), Caribbean tropical region (Bunt et al., 1972), Adriatic Sea (Blackford, 2002), and Chukchi Sea (Matheke and Horner, 1974), the contribution of benthic microalgae (mainly diatoms) is reported to be approximately 50 % of the annual net primary production, indicating that they contribute substantially to primary production in coastal areas, lagoons, and estuaries. In Hokkaido, the contribution of benthic microalgae to the total primary production at Mombetsu Port during the winter season covered by sea ice is up to 64.5 % (McMinn et al., 2005). Therefore, benthic/sessile diatoms are suggested to actively photosynthesize and may contribute to primary production in the water column around Hakodate Bay, even for a limited period.

4.5. Dominance of Thalassiosira spp. in the winter group

The Winter group mainly occurred from late November to early March with *Thalassiosira* spp. being dominant. The average water temperature was significantly lower (8.0°C) than that during the occurrence of the other groups. As *Thalassiosira* spp. are adapted to low temperatures (Durbin, 1974), the low water temperature in the Hakodate Bay is speculated to have presented a suitable condition for *T. gravida* and *T. nordenskioeldii*, which were the dominant species in the Winter group. The half-saturation constant of nitrate uptake is high for large species and low for small species (Eppley et al., 1969). The half-saturation constants on nitrate uptake of *T. gravida* and *T. nordenskioeldii* are estimated to be 2.3−2.5 μM (Waite et al., 1992). The nitrate concentration during the occurrence period of the Winter group was in the range of 4.5–24.0 μM, and sufficient nitrate was present to exceed the half-saturation constant of *T. gravida* and *T. nordenskioeldii*, which implies that their nutrient uptake and growth were not limited.

Regarding photosynthesis activity, *Fv/Fm* is affected by temperature, irradiance, nutrients (Björkman and Demmig, 1987; Goto et al., 2008). Low *Fv/Fm* in the winter group maybe caused by low temperature (8.0 ±3.74°C) and low irradiance (750±350 μmol m^{-2} s^{-1} at the sampling timing during the winter group) rather than nutrients, as mentioned above. High *ETRm* was also seen, which means high potential primary production, but the primary production maybe low due to the low PPFD. Thus, phytoplankton cells were not healthy and primary production was restricted by low light intensity, resulting in low cell density.

Thalassiosira nordenskioeldii is an important species that forms spring blooms in the Funka Bay, Hokkaido (Nakata, 1981; Odate, 1987; Shinada et al., 1999). According to Shinada et al. (1999), the origin of the spring bloom of *Thalassiosira* spp. in the Funka Bay is the cell transport by Oyashio water (Oyashio water and Coastal Oyashio water) rather than resting spores in the bay. In 1994, when no inflow of Oyashio water was observed in the Funka Bay, *Chaetoceros* spp. dominated the early spring blooms (Shinada et al., 1999). Oyashio water is characterized as having temperature below 7°C, salinity 33.0–33.7, and density below 26.7; Coastal Oyashio water is characterized as having temperature below 2°C and salinity below 33.0 (Hanawa and Mitsudera, 1987). Coastal Oyashio water flows into the southern shelf of Hokkaido (Hidaka Bay) from February to March every year (Isoda et al., 2003). Because Coastal Oyashio water occasionally reaches Hakodate Bay during winter (Ohtani, 1987), it is possible that Coastal Oyashio water flowed into the sampling area. On checking the water temperature and salinity during the occurrence of the Winter group, 13 water samples (50 % of the Winter group) were determined to be Oyashio water. However, the water mass was confirmed much earlier than the previously reported inflow of Oyashio water, and it is difficult to distinguish whether water masses with characteristics similar to those of the Oyashio water were formed because of the cooling of the sea surface and precipitation. Therefore, further studies are required regarding the inflow of water from the Oyashio system, including physical observations around the Hakodate Bay and water mass classifications based on more stable chemical parameters.

4.6. Characteristics of the spring group

Relatively high *Fv/Fm* was seen in the Spring group, as well as the Benthic group. From winter to spring, temperature increased from 8.0°C to 11.9°C, and solar radiation was drastically increased from 8.7 to 16.4 MJ m^{-2} day^{-1}. These favorite conditions for phytoplankton photosynthetic activity reduce the stress in cells and prepare for spring bloom (Björkman and Demmig, 1987).

The Spring group occurred alternately with the Benthic group and was characterized by the dominance of pelagic and planktonic diatoms, including *Chaetoceros* spp. Comparing the environmental parameters between the Benthic and Spring groups, significant differences were observed in wind speed and turbidity; the average wind speed was 3.6 m s^{-1} and 2.9 m s^{-1} in the Benthic and Spring groups, respectively, and the turbidity was 23.8 FTU and 9.0 FTU in the Benthic and Spring groups, respectively. Therefore, in the spring in the Hakodate Bay, when the sea is agitated by strong winds, the Benthic group (dominated by benthic and sessile diatoms) occurs, and when the wind is weak and sea conditions are stable, the Spring group (dominated by pelagic and planktonic diatoms) occurs.

In the waters around Hokkaido, a transition of the dominant species from *Thalassiosira* spp. to *Chaetoceros* spp. from late winter to early spring is known in the Funka Bay (Nakata, 1981; Odate, 1987; Shinada et al., 1999) and Mombetsu Port (Matsumoto et al., 2021). This transition is consistent with the results of our study in the Hakodate Bay. In addition to coastal areas, in the open ocean of the subarctic North Pacific, *Thalassiosira* spp., including *T. nordenskioeldii*, dominate in April, followed by *Chaetoceros* spp., which is classified as a *Hyalochate* (Sugie et al., 2010), *Thalassiosira pacifica,* and *T. nordenskioeldii* are dominant in June–July, but from August onwards, *C. debilis* and *Chaetoceros concavicornis* are dominant (Mochizuki et al., 2002). Thus, this spring species transition is considered a common phenomenon not only in the Hokkaido coastal area but also in the subarctic North Pacific region.

4.7. Occurrence of harmful dinoflagellate Karenia mikimotoi group

The *Karenia* group occurred only from late August 2021 to early January 2022 and was characterized by the diatoms *M. varians* and *Navicula* spp., dinoflagellate *K. mikimotoi*, and oligotrich ciliates. Regarding nutrients, it is speculated that sufficient nutrients (DIN from 6.8−25.0 μM and phosphate from 0.51−1.2 μM) were available for *K. mikimotoi* to grow during this period because the half-saturation constant of *K. mikimotoi* is 0.78 μM for DIN and 0.14 μM for phosphate (Yamaguchi, 1994). The growth rate of *K. mikimotoi* is sensitive to temperature changes (Yamaguchi and Honjo, 1989), and approximately 10°C is suggested to be a growth-limiting factor in the Hakodate Bay

(Kakumu et al., 2018). In the present study, the water temperature during the occurrence of the *Karenia* group was 6.1–25.3°C (average 14.0°C), and their occurrence was confirmed even at a low temperature of 6.1°C. Based on field sampling and morphological observation of *K. mikimotoi* during winter in the Suo-Nada Sea of the Seto Inland Sea, *K. mikimotoi* cannot survive at <4°C; however, they possibly overwinter at 6.5–9.0°C (Terada et al., 1987). The lowest water temperature in the Hakodate Bay was 4.5°C observed on January 31, 2022; however, in the future, if the winter water temperature rises to 6.0°C or higher owing to global warming, *K. mikimotoi* will overwinter.

As a characteristic interannual difference, *K. mikimotoi* occurred from late August 2021 to early January 2022, but not during the same period as in the previous year. In Uwajima Bay, Ehime Prefecture, Japan, the bottom layer DIN concentration in *K. mikimotoi* bloom years was higher than that in non-bloom years, and ammonia nitrogen accounted for most of the concentration difference (68–85 %) between the years (Onitsuka et al., 2021). *Karenia mikimotoi* can utilize nitrate, ammonia, and urea as nitrogen sources. For nitrate and ammonia, an increase in *in-vivo* chlorophyll fluorescence and a prolonged logarithmic growth phase have been observed with increasing concentrations (Yamaguchi, 1994). In the present study, ammonium concentration during the occurrence of the *K. mikimotoi* group (from late August 2021 to early January 2022) was higher (7.06 μM) than that in the same period in the previous year (4.94 μM). These findings suggest that an increase in ammonium may have contributed to the occurrence of the *Karenia* group in the autumn and winter of 2021. Total solar radiation (average 8.4 MJ m^{-2}) and daylight hours (average 4.4 h) during the occurrence of the *Karenia* group were both the lowest among all the groups. It is possible that weather during this period was cloudy. Laboratory experiments have revealed that *K. mikimotoi* can grow under lower PPFD than other dinoflagellates (Yamaguchi and Honjo, 1989). According to field observations, *K. mikimotoi* is more likely to bloom on cloudy days than are other dinoflagellates (Yanagi et al., 1992). In contrast, light intensity strongly influences the growth of diatoms, which are competitors of *K. mikimotoi*, and the average total solar radiation of 13.3 MJ m^{-2} is the limit for the growth of diatoms (Erga and Heimdal, 1984). During the period when the *Karenia* group did not appear (September 3, 2020 to January 13, 2021), the total solar radiation was 15.2 MJ m^{-2} and 13.8 MJ m^{-2} in the Summer and Benthic groups, respectively; these results suggest the diatoms were not subject to light limitation. Therefore, from late August 2021 to early January 2022, clouds continued to limit the growth of diatoms, resulting in the proliferation of low light-adapting *K. mikimotoi* by using nutrients (especially ammonium).

In the Hakodate Bay, the *K. mikimotoi* bloom was first observed in 2015 and has since been frequently observed. Transport by the Tsushima–Tsugaru warm currents may have been the cause (Shimada et al., 2016; Kakumu et al., 2018). During the *K. mikimotoi* bloom in Hakodate Bay in 2015, the highest cell density was 1.15×10^7 cells L^{-1} (Shimada et al., 2016) and 6.3×10^5 cells L^{-1} (Kakumu et al., 2018), which are densities similar to our result (maximum 6.29×10^5 cells L^{-1}). However, in these two previous studies, *K. mikimotoi* did not occur by mid-December, whereas in our study, it occurred until mid-January, indicating that the occurrence period was one month longer. In 2015, the day when the water temperature dropped to approximately 10°C, which limits the growth of *K. mikimotoi*, was November 28th; however, in the present study, it was December 20th. This difference may have extended the occurrence period of *K. mikimotoi*. In the future, as there is a possibility that the occurrence of *K. mikimotoi* blooms will increase, and the period will become longer owing to the remarkable global warming trend, continuous investigation is required.

5. Conclusion

Seasonal changes in the protist community in Hakodate Bay were observed over two years, along with changes in species composition. Because the Winter, Summer, and Spring groups occur in both years, they are considered the basic community in the bay. The Winter group showed low photosynthetic activity with the dominance of low-temperature-adapted *Thalassiosira* spp., which was partly attributed to the inflow of Coastal Oyashio water. Following the Winter group, the Spring group exhibited a dominance by *Chaetoceros* spp. with high *Fv/Fm*. This species transition from *Thalassiosira* spp. to *Chaetoceros* spp. between winter and spring and increasing photosynthetic activity are considered a phenomenon widely observed in the subarctic region as spring blooms. In summer, because the environment was prone to fluctuations owing to the inflow of warm, high-salinity Tsugaru Warm water and decreasing salinity by precipitation, high salinity-tolerant species (diatoms *L. danicus* and *S. costatum* and dinoflagellate *Prorocentrum* spp.) were present in the Summer group. The highest *Fv/Fm* was seen due to high irradiance, high nutrients and warm temperature. The Late Spring, Benthic, and *Karenia* groups occurred randomly, filling the spaces between the three previously mentioned groups. The Late Spring group was observed in May, June, and October, and was characterized by high densities of dinoflagellate *Scrippsiella* spp. This was probably because the cysts of *Scrippsiella* spp., which accumulated around Hakodate Bay, germinated and grew under the optimal water temperature, and are accumulated by wind-driven currents. The Benthic group occurred in spring and autumn, and was dominated by benthic and sessile diatoms such as *Navicula* spp. Since the benthic species had a strong relationship with wind speed and turbidity, the group was made up of strong winds that caused rough sea conditions and the release of benthic and sessile diatoms into the water. The *Karenia* group was observed only from late August 2021 to early January 2022, when higher ammonium and lower light conditions were detected compared to the same period last year. Owing to environmental conditions, the growth of diatoms was restricted by low light intensity, whereas the population of *K. mikimotoi* increased by taking advantage of the abundant nutrients in the autumn and winter of 2021. Since nutrients were not depleted throughout the year, the stress in phytoplankton cells and photosynthetic activity are mainly controlled by the seasonality of temperature and irradiance in the Hakodate Bay. Seasonal changes in the protist community in the Hakodate Bay can generally be explained by water temperature; however, in the short term (1–2 weeks), they are also influenced by meteorological conditions (solar radiation, wind, and precipitation). These findings will help improve our understanding of the impacts of climate change on productivity and the mechanisms of protists in coastal areas.

CRediT authorship contribution statement

Shoko Tatamisashi: Investigation, Formal analysis, Data curation. **Yusuke Hamao:** Writing – original draft, Visualization, Formal analysis, Data curation. **Kyosei Morimoto:** Investigation, Formal analysis. **Kohei Matsuno:** Writing – review & editing, Supervision, Methodology, Funding acquisition, Formal analysis, Conceptualization. **Masahide Wakita:** Investigation, Conceptualization. **Akihide Kasai:** Investigation, Formal analysis, Conceptualization.

Declaration of Competing Interest

The authors declare that they have no known competing financial interests or personal relationships that could have appeared to influence the work reported in this paper.

Data Availability

Data will be made available on request.

Acknowledgments

This work was supported by the Japan Society for the Promotion of

Science (JSPS) KAKENHI [grant number JP21H02263 (B)].

Appendix A. Supporting information

Supplementary data associated with this article can be found in the online version at doi:10.1016/j.rsma.2024.103775.

References

Al-Yamani, F.Y., Saburova, M.A., 2011. Illustrated guide on the benthic diatoms of Kuwait's marine environment. Kuwait Institute for Scientific Research, Kuwait.

Anderson, D.M., 1984. Shellfish toxicity and dormant cysts in toxic dinoflagellate bloom. In: Ragelis, E.P. (Ed.), Seafood toxins. American Chemical Society, Washington, D.C., pp. 125–138

Bi, H., Song, J., Zhao, J., Liu, H., Cheng, X., Wang, L., Cai, Z., Benfield, M.C., Otto, S., Goberville, E., Keister, J., Yang, Y., Yu, X., Cai, J., Ying, K., Conversi, A., 2022. Temporal characteristics of plankton indicators in coastal waters: High-frequency data from PlanktonScope. J. Sea Res. 189, 102283.

Björkman, O., Demmig, B., 1987. Photon yield of O_2 evolution and chlorophyll fluorescence characteristics at 77K among vascular plants of diverse origins. Planta 170, 489–504.

Blackford, J.C., 2002. The influence of microphytobenthos on the northern Adriatic ecosystem, a modeling study. Est. Coast. Shelf Sci. 55, 109–123.

Bricaud, A., Babin, M., Morel, A., Claustre, H., 1995. Variability in the chlorophyll-specific absorption coefficients of natural phytoplankton: analysis and parameterization. J. Geophys. Res. Oceans 100, 13321–13332.

Brzezinski, M.A., 1985. The Si:C:N ratio of marine diatoms: inter-specific variability and the effect of some environmental variables. J. Phycol. 21, 347–357.

Buchel, C., Wilhelm, C., 1993. *In vivo* analysis of slow chlorophyll induction kinetics in algae: progress, problems and perspectives. Phtochem. Photobiol. 58, 137–148.

Bunt, J.S., Lee, C.C., Lee, E., 1972. Primary production and related data from tropical and subtropical marine sediments. Mar. Biol. 16, 28–36.

Cadée, G.C., Hegeman, J., 1974. Primary production of the benthic microflora living on tidal flats in the Dutch Wadden Sea. Neth. J. Sea Res. 8, 260–291.

Dickey, T., Zedler, S., Yu, X., Doney, S.C., Frye, D., Jannasch, H., Manov, D., Sigurdson, D., McNeil, J.D., Dobeck, L., Gilboy, T., Bravo, C., Siegel, D.A., Nelson, N., 2001. Physical and biogeochemical variability from hours to years at the bermuda testbed mooring site: June 1994–March 1998. Deep Sea Res. II 48, 2105–2140.

DiTullio, G.R., Gremeler, J.M., Arrigo, K.R., Lizzotte, M.P., Robinson, D.H., Leventer, A., Barry, J.P., VanWoert, M.L., Dunbar, R.B., 2000. Rapid and early export of *Phaeocystis antarctica* blooms in the Ross Sea, Antarctica. Nature 404, 595–598.

Dufréne, M., Legendre, P., 1997. Species assemblages and indicator species: the need for a flexible asymmetrical approach. Ecol. Monogr. 67, 345–366.

Durbin, E.G., 1974. Studies on the autecology of the marine diatom *Thalassiosira nordenskioeldii* cleve. 1. the influence of day length, light intensity, and temperature on growth. J. Phycol. 10, 220–225.

Egge, J.K., 1998. Are diatoms poor competitors at low phosphate concentration? J. Mar. Syst. 16, 191–198.

Elbrachter, M., 1991. Food uptake mechanism in phagotrophic dinoflagellates and classification. In: Patterson, D.J., Larsen, J. (Eds.), The Biology of Free-living Heterotrophic Flagellates, Systematics Association Special Volume 45, Clarendon Press. Oxford, pp. 303–312.

Eppley, R.W., Rogers, J.N., McCarthy, J.J., 1969. Half-saturation constants for uptake of nitrate and ammonium by marine phytoplankton. Limnol. Oceanogr. 14, 912–920.

Erga, S.R., Heimdal, B.R., 1984. Ecological studies on the phytoplankton of Korsfjorden, western Norway. The dynamics of a spring bloom seen in relation to hydrographical conditions and light regime. J. Plankton Res. 6, 67–90.

Fukui, D., Kitatsuji, S., Ikeda, T., Shiga, N., Yamaguchi, A., 2010. Long-term changes in the abundance and community structure of net-phytoplankton in Oshoro Bay, Hokkaido. Bull. Plankton Soc. Jpn. 57, 30−−340.

Fukuyo, Y., Inoue, H., Takayama, H., 1997. Division dinophyta. an illustrated guide to marine plankton in Japan. Tokai University Press, pp. 31–146.

Giesbrecht, K.E., Varela, D.E., Wiktor, J., Grebmeier, J.M., Kelly, B., Long, J.E., 2019. A decade of summertime measurements of phytoplankton biomass, productivity and assemblage composition in the Pacific Arctic Region from 2006 to 2016. Deep-Sea Res. II 162, 93–113.

Goto, N., Kihira, M., Ishida, N., 2008. Seasonal distribution of photosynthetically active phytoplankton using pulse amplitude modulated fluorometry in the large monomictic Lake Biwa, Japan. J. Plankton Res. 30, 1169–1177.

Hanawa, K., Mitsudera, H., 1987. Variations of water system distribution in the Sanriku coast area. J. Oceanogr. Soc. Jpn. 42, 435–446.

Hargraves, P.E., French, F.W., 1983. Diatom resting spore: significance and strategies. In: Fryxell, G.A. (Ed.), Survival strategies of the Algae. Cambridge University Press, Cambridge, pp. 49–68.

Hasle, G.R., Syvertsen, E.E., 1997. Marine diatoms. In: Tomas, C.R. (Ed), Identifying marine phytoplankton. Academic Press, San Diego, pp. 5–385.

Herberich, E., Sikorski, J., Hothorn, T., 2010. A robust procedure for comparing multiple means under heteroscedasticity in unbalanced designs. PLoS One 5, e9788. https://doi.org/10.1371/journal.pone.0009788.

Holm-Hansen, O., Lorenzen, C.J., Holms, R.W., Strickland, J.D.H., 1965. Fluorometric determination of chlorophyll. J. Mar. Sci. 30, 3–15.

Horner, R.A., 2002. A taxonomic guide to some common marine phytoplankton. Biopress Limited, United Kingdom.

Isoda, Y., Kuroda, H., Myousyo, T., Honda, S., 2003. Hydrographic feature of Coastal Oyashio and its seasonal variation. Bull. Coast. Oceanogr. 41, 5–12.

Itakura, S., 2000. Physiological ecology of the resting stage cells of coastal planktonic diatoms. Bull. Fish. Environ. Inland Sea 2, 67–130.

Johnsen, G., Sakshang, E., 2007. Biooptocal characterristics of PSII and PSI in 33 species (13 pigment groups) of marine phytoplankton, and the relevance for pulse-amplitude-modulated and fast-repetition-rate fluorometry. J. Phycol. 43, 1236–1251.

Justic, D., Rabalais, N.N., Turner, R.E., 1995. Stoichiometric nutrient balance and origin of coastal eutrophication. Mar. Pollut. Bull.. 38, 41–46.

Kakumu, A., Morita, K., Shimada, H., Yamagichi, A., Imai, I., 2018. First detection of the noxious red tide dinoflagellate *Karenia mikimotoi* and bloom dynamics in 2015 and 2016 in Hakodate Bay, Hokkaido, northern Japan. Bull. Plankton Soc. Jpn. 65, 1–11.

Karthik, R., Padmavati, G., Elangovan, S.S., Sachithanandam, V., 2017. Monitoring the diatom bloom of *Leptocylindrus danicus* (Cleve 1889, Bacillariophyceae) in the coastal waters of South Andaman Island. Indian J. Geo Mar. Sci. 46, 958–965.

Kida, S., Takayama, K., Sasaki, Y.N., Matsuura, H., Hirose, N., 2021. Increasing trend in Japan Sea throughflow transport. J. Oceanogr. 77, 145–153.

Li, Y., Lu, S., Jiang, T., Xiao, Y., You, S., 2011. Environmental factors and seasonal dynamics of *Prorocentrum* populations in Nanji islands national nature reserve, East China Sea. Harmful Algae 10, 426–432.

Liu, H., Song, X., Huang, L., Tan, Y., Zhang, J., 2011. Phytoplankton biomass and production in northern South China Sea during summer: influenced by Pearl River discharge and coastal upwelling. Acta Ecol. Sin. 31, 133–136.

Matheke, G.E., Horner, R., 1974. Primary productivity of the benthic microalgae in the Chukchi Sea near Barrow, Alaska. J. Fish. Res. Board Can. 31, 1279–1286.

Matsumoto, T., Matsuno, K., Katakura, S., Kasai, H., Yamaguchi, A., 2021. Seasonal variability of the protist community and production in the southern Okhotsk Sea revealed by weekly monitoring. Reg. Stud. Mar. Sci. 43, 101683.

McMinn, A., Hirawake, T., Hamaoka, T., Hattori, H., Fukuchi, M., 2005. Contribution of benthic microalgae to ice covered coastal ecosystems in northern Hokkaido, Japan. J. Mar. Biol. Ass. U. K. 85, 283–289.

McQuoid, M.R., Hobson, L.A., 1996. Diatom resting stages. J. Phycol. 32, 889–902.

Miyatake, M., Yoshie, Y., Minato, K., Matsumura, K., 2011. Variation characteristics of tidal current and water quality in Hakodate port. J Jpn. Soc. Civ. Eng. Ser. B3 (Ocean Eng.) 67, 322–327.

Miyazono, A., Shimada, H., 2000. Population dynamics of dinoflagellates after diatom bloom and environmental factors. Bull. Coast. Oceanogr. 38, 29–38.

Mochizuki, M., Shiga, N., Saito, M., Imai, K., Nojiri, Y., 2002. Seasonal changes in nutrients, chlorophyll *a* and the phytoplankton assemblage of the western subarctic gyre in the Pacific Ocean. Deep-Sea Res. II 49, 5421–5439.

Morgan-Kiss, R.M., Priscu, J.C., Pocock, T., Gudynaite-Savitch, L., Huner, N.P.A., 2006. Adaptation and acclimation of photosynthetic microorganisms to permanently cold environments. Microbiol. Mol. Biol. Rev. 70, 222–252.

Nakagami, M., Takatsu, T., Nakaya, M., Takahashi, T., 2001. Spatial and temporal distribution of larval and juvenile Marbled Sole *Pleuronectes yokohamae* in Hakodate Bay. Bull. Jpn. Soc. Fish. Oceanogr. 65, 85–93.

Nakata, K., 1981. Species composition of phytoplankton community of Funka Bay in the spring bloom. Bull. Jpn. Soc. Fish. Oceanogr. 41, 27–32.

Natsuike, M., Kanamori, M., Shimada, H., 2019. Red tide and seasonal occurrence of the harmful raphidophyte *Heterosigma akashiwo* in Hakodate Bay. Hokkaido. Sci. Rep. Hokkaido Fish. Res. Inst. 95, 11–17.

Natsuike, M., Kanamori, M., Sugawara, A., Sakamoto, S., 2021. Effects of water temperature, salinity, and irradiance on growth and toxin profiles of the dinoflagellate *Alexandrium pacificum* isolated from Hakodate and Funka Bays, Hokkaido, Japan. Bull. Plankton Soc. Jpn. 68, 1–10.

Nishida, Y., Kanomata, I., Tanaka, I., Sato, S., Takahashi, S., Matsubara, H., 2003. Seasonal and interannual variations of the volume transport through the Tsugaru Strait. Oceanogr Jpn 12, 487–499.

Nishikawa, T., Hori, Y., Nagai, S., Miyahara, K., Nakamura, Y., Harada, M., Tanda, M., Manabe, T., Tada, K., 2010. Nutrients and phytoplankton dynamics in Harima-Nada, eastern Seto Inland Sea, Japan during a 35-year period from 1973 to 2007. Estuar. Coasts 33, 417–427.

Odate, T., 1987. Temporal and horizontal distribution of the diatom community during the spring bloom in Funka Bay, southern Hokkaido. Bull. Plankton Soc. Jpn. 34, 33–42.

Odate, T., Miyazono, A., Yanada, M., Yagi, H., Maita, Y., 1993. Vertical distribution of phytoplankton and ciliates in Iwanai Bay, spring 1988. Bull. Coast. Oceanogr. 30, 194–200.

Oh, S.J., Matsuyama, Y., Yamamoto, T., Nakajima, M., Takatyuzi, H., Hujisawa, K., 2005. Recent developments and causes of harmfu1 dinoflagellate blooms in the Seto lnland sea ecological importance of dissolved organic phosphorus (DOP). Bull. Coast. Oceanogr. 43, 85–95.

Ohara, S., Yano, R., Hagiwara, E., Yoneyama, H., Koike, K., 2020. Environmental and seasonal dynamics altering the primary productivity in Bingo-Nada (Bingo Sound) of the Seto Inland Sea, Japan. Plankton Benthos Res 15, 78–96.

Ohtani, K., 1987. Westward inflow of the coastal oyashio water into the Tsugaru Strait. Bull. Fish. Sci. Hokkaido Univ. 38, 209–220.

Olli, K., Heiskanen, A.S., Seppala, J., 1996. Development and fate of *Eutreptoella gymnastica* bloom in nutrient-enriched enclosures in the coastal Baltic Sea. J. Plankton Res. 18, 1587–1604.

Onitsuka, G., Suzukawa, K., Yoshie, N., Hirai, M., Takenaka, S., Yoshihara, Y., Ohnishi, H., Shimizu, S., Takeuchi, H., Ohta, K., Tomaru, Y., Sakamoto, S., Abe, K., Yamaguchi, A., Shikata, T., Yamaguchi, H., Takeoka, H., 2021. Spatio-temporal dynamics of the harmful dinoflaagellate *Karenia mikimotoi* in Uwajima Bay and its

adjacent waters: comparison between a bloom occurrence year and a non-occurrence year. Nippon Suisan Gakkaishi 87, 144–159.
Parsons, T.R., Takahashi, M., Hargrave, B.,1984. Biological Oceanographic Processes 3rd. Edition. Butterworth-Heinemann, Oxford.
Quinn, G.P., Keough, M.J., 2002. Experimental design and data analysis for biologists. Cambridge University Press, New York.
R Core Team, 2021. R: A language and environment for statistical computing. R Foundation for Statistical Computing, Vienna, Austria. https://www.R-project.org/.
Raymont, J.E.G., 1980. Plankton and productivity in the oceans. Pergamon Press, Oxford.
Redfield, A.C., Ketchum, B.H., Richards, F.A., 1963. The influence of organisms on the composition of seawater. In: Hill, M.N. (Ed.), The Sea. John Wiley, New York, pp. 26–77.
Sanders, R.W., 1991. Trophic strategies among heterotrophic flagellates. In: Patterson, D. J., Larsen, J. (Eds.), The Biology of Free-living Heterotrophic Flagellates, Systematics Association Special Volume 45, Clarendon Press. Oxford, pp. 21–38.
Sato, S., 2001. Estimate of condition on Tsushima-warm current. Bull. Aomori Pref. Fish. Exp. Stn. 1, 17–26.
Schreiber, U., Bilger, W., Neubauer, C., 1995. Chlorophyll fluorescence as a non-intrusive indicator for rapid assessment of *in vivo* photosynthesis. In: Schulze, E.D., Caldwell, M.M. (eds) Ecophysiology of Photosynthesis. Springer Study Edition, vol 100. Springer, Berlin, Heidelberg.
Schreiber, U., Schliwa, U., Bilger, W., 1986. Continuous recording of photochemical and non-photochemical chlorophyll fluorescence quenching with a new type of modulation fluorometer. Photosynth. Res. 10, 51–62.
Sergeeva, V.M., Sukhanova, I.N., Flint, M.V., Pautova, L.A., Grebmeir, J.M., Cooper, L. W., 2010. Phytoplankton community in the western Arctic in July−August 2003. Oceanology 50, 184–197.
Sherr, E.B., Sherr, B., 1988. Role of microbes in pelagic food webs: a revised concept. Limnol. Oceanogr. 33, 1225–1227.
Shimada, H., 2021. Long-term fluctuation of red tide and shellfish toxin along the coast of Hokkaido (Review). Sci. Rep. Hokkaido Fish. Res. Inst. 100, 1–12.
Shimada, H., Kanamori, M., Yoshida, H., Imai, I., 2016. First record of red tide due to the harmful dinoflagellate *Karenia mikimotoi* in Hakodate Bay, southern Hokkaido, in autumn 2015. Nippon Suisan Gakkaishi 82, 934–938.
Shinada, A., Shiga, N., Ban, S., 1999. Structure and magnitude of diatom spring bloom in Funka Bay, southwestern Hokkaido, Japan, as influenced by the instruction of Coastal Oyashio Water. Plankton Biol. Ecol.. 46, 24–29.
Steidinger, K.A., 1993. Some taxonomic and biologic aspects of toxic dinoflagellates, In: Falconer, I.R. (Ed.), Algal Toxins in Seafood and Drinking Water, Academic Press, London, pp. 1−28.
Steidinger, K.A., Tangen, K., 1997. Dinoflagellates. In: Tomas, C.R. (Ed.), Identifying marine phytoplankton. Academic Press, San Diego, pp. 387–584.
Stoecker, D.K., Gifford, D.J., Putt, M., 1994. Preservation of marine planktonic ciliates: losses and cell shrinkage during fixation. Mar. Ecol. Prog. Ser. 110, 293–299.
Sugie, K., Kuma, K., Fujita, S., Ikeda, T., 2010. Increase in Si:N drawdown ratio due to resting spore formation by spring bloom-forming diatoms under Fe- and N-limited conditions in the Oyashio region. J. Exp. Mar. Biol. Ecol.. 382, 108–116.
Sugimoto, R., Kasai, A., Tait, D.R., Rihei, T., Hirai, T., Asai, K., Tamura, Y., Yamashita, Y., 2021. Traditional land use effects on nutrient export from watersheds to coastal seas. Nutr. Cycl. Agroecosyst. 119, 7–21.
Tadokoro, K., Sugimoto, T., Kishi, M., 2008. The effects of anthropogenic global warming on the marine ecosystem. Oceanogr. Jpn. 17, 404–420.
Terada, K., Ikeuchi, H., Takayama, H., 1987. Winter distribution of *Gymnodinium nagasakiense* (Dinophyceae) in coastal waters of Suo-Nada, Inland Sea of Japan. Bull. Plankton Soc. Jpn. 34, 201–204.
Thom, R.M., Albright, R.G., 1992. Dynamics of benthic vegetation standing stock, irradiance and water properties in central Puget Sound. Mar. Biol. 104, 129–141.
Throndsen, J., 1997. The planktonic marine flagellates. In: Tomas, C.R. (Ed), Identifying marine phytoplankton. Academic Press, San Diego, pp. 591–715.
Tian, Y., Hu, S., Lin, X., Huang, H., Song, X., Yan, Y., Xie, X., Li, T., Liu, S., 2021. Mechanisms of high-frequency dinoflagellate blooms of *Scrippsiella trochoidea* in Daya Bay, South China Sea. Chin. J. Oceanol. Limnol. 39, 1293–1304.
Turpin, D.H., Harrison, P.J., 1980. Cell size manipulation in natural marine planktonic diatom communities. Can. J. Fish. Aquat. Sci. 37, 1193–1195.
Uchida, T., 1994. Effects of temperature on the encystment and excystment of a Dinoflagellate *Scrippsiella trochoida* isolated from Muroran Harbor, Hokkaido. Bull. Nansei Natl. Fish. Res. Inst. 27, 243–249.
Waite, A., Bienfang, P.K., Harrison, P.J., 1992. Spring bloom sedimentation in a subarctic ecosystem. Mar. Biol. 114, 119–129.
Wakita, M., Sasaki, K., Nagano, A., Abe, H., Tanaka, T., Nagano, K., Sugie, K., Kaneko, H., Kimoto, K., Okunishi, T., Takada, M., Yoshino, J., Watanabe, S., 2021. Rapid reduction of pH and $CaCO_3$ saturation state in the Tsugaru Strait by the intensified Tsugaru Warm Current during 2012−2019. e2020GL091332 Geophys. Res. Lett. 48. https://doi.org/10.1029/2020GL091332.
Wall, D., 1971. Biological problems concerning fossilizable dinoflagellates. Geosci. Man. 3, 1–15.
Wei, H., Sun, J., Moll, A., Zhao, L., 2004. Phytoplankton dynamics in the Bohai Sea-observation and modeling. J. Mar. Syst. 44, 233–251.
Yamada, M., 2013. Recent studies on biodiversity and eco-physiological characteristics of the genus *Skeletonema* (Bacillariophyceae). Bull. Plankton Soc. Jpn. 60, 18–28.
Yamaguchi, M., 1994. Physiological ecology of the red tide flagellate Gymnodinium nagasakiense (Dinophyceae) – Mechanism of the red tide occurrence and its prediction. Bull. Nansei Natl. Fish. Res. Inst. 27, 251–394.
Yamaguchi, M., Honjo, T., 1989. Effects of temperature, salinity and irradiance on the growth of the noxious red tide flagellate *Gymnodinium nagasakiense* (Dinophyceae). Nippon Suisan Gakkaishi 55, 2029–2036.
Yanagi, T., Asai, Y., Koizumi, Y., 1992. Physical conditions for red tide outbreak of *Gymnodinium mikimotoi*. Bull. Jpn. Soc. Fish. Oceanogr. 56, 107–112.
Yasui, T., Abe, H., Hirawake, T., Sasaki, K.I., Wakita, M., 2022. Seasonal pathways of the Tsugaru Warm Current revealed by high-frequency ocean radars. J. Oceanogr. 78, 103–119.
Yin, K., Song, X., Liu, S., Kan, J., Qian, P., 2008. Is inorganic nutrient enrichment a driving force for the formation of red tides? A case study of the dinoflagellate *Scrioosiella trochoidea* in an embayment. Harmful Algae 8, 54–59.
Zuur, A.F., Ieno, E.N., Walker, N.J., Saveliev, A.A., Smith, G.M., 2009. Mixed effects models and extensions in ecology with R. Springer, New York.